

Effects of geometrical and energetic nonadditivity on the phase behavior of two-component symmetric mixtures

A. Patrykiewicz*

Department for the Modelling of Physico-Chemical Processes, Faculty of Chemistry, MCS University, 20031 Lublin, Poland

(Received 4 October 2016; published 23 January 2017)

Using Monte Carlo simulation methods in the grand-canonical ensemble, we have studied the phase behavior of three-dimensional symmetric binary mixtures of Lennard-Jones particles. We have also elucidated the effects of geometric and energetic nonadditivity on the phase behavior. Phase diagrams for several systems have been evaluated. We have demonstrated that in completely miscible mixtures the geometrical nonadditivity (negative as well as positive) stabilizes a liquid phase leading to a gradual increase of the critical temperature. The mechanism leading to such behavior is different when the system shows negative and positive geometrical nonadditivity. In the case of systems with negative energetic nonadditivity, which may exhibit demixing transition in the liquid phase, their phase behavior is also strongly affected by the geometric non-additivity. The systems with negative geometric nonadditivity have been demonstrated to show reentrant miscibility, while those with positive geometric nonadditivity show enhanced tendency toward mixing at sufficiently high temperatures. We have evaluated phase diagrams for several systems.

DOI: [10.1103/PhysRevE.95.012145](https://doi.org/10.1103/PhysRevE.95.012145)

I. INTRODUCTION

Binary mixtures are known to exhibit a complex phase behavior [1–3]. Even a very simple model of symmetric binary mixture (SBM) has been found to show demixing transitions in the liquid and solid phases [3–6] and reentrant miscibility [7,8]. One recalls that a symmetric mixture consists of two identical components, A and B. The interaction between the like particles, A-A and B-B, are the same, and only the A-B interaction differs. Generally speaking, one can assume that the pair interaction potential depends on two parameters. One of them (ε) specifies the strength of interaction and the other (σ) determines the range of the interaction. In binary mixtures, one has to include the interactions between different pairs, A-A, B-B, and A-B, resulting in six parameters specifying the interactions: ε_{AA} , ε_{AB} , ε_{BB} , σ_{AA} , σ_{AB} , and σ_{BB} . In additive mixtures, one usually uses Berthelot mixing rules and assumes that $\varepsilon_{AB} = \sqrt{\varepsilon_{AA}\varepsilon_{BB}}$ and $\sigma_{AB} = (\sigma_{AA} + \sigma_{BB})/2$. In the case of symmetrical mixtures, $\varepsilon_{AA} = \varepsilon_{BB}$ and $\sigma_{AA} = \sigma_{BB}$, so the additivity principle leads to a rather uninteresting case of an ideal mixture. Therefore, one can assume that symmetrical mixtures are nonadditive, so ε_{AB} and σ_{AB} can take on some arbitrarily chosen values.

A vast majority of the previously published results for SBMs [3,9–12] has been devoted to the understanding of the demixing transition in the liquid phase resulting from the weakening of the interaction strength between the unlike particles, i.e., $\varepsilon_{AB} < \varepsilon_{AA}$, while σ_{AB} has been assumed to be equal to σ_{AA} . It has been demonstrated that different phase diagram topologies are possible [3,4]. In particular, theoretical studies based on the mean-field and the Ginsburg-Landau approaches as well as Monte Carlo simulation [3] have allowed us to single out four types of phase diagrams within the temperature and density regions over which only fluid phases (vapor and liquids) are present. When the interactions in the system are such that the liquid phase is mixed over the entire

range of temperatures, the phase diagram is qualitatively the same as in the case of one-component systems. Thus, the gas-liquid coexistence terminates in the critical point. The situation becomes more complex when the interaction between the unlike particles is weaker than the interaction between the like particles. In such cases, the liquid phase may undergo a demixing transition. When ε_{AB} is only slightly lower than ε_{AA} , the demixing transition occurs only at the temperatures below the triple point, in the solid phase, while the liquid is mixed over the entire range of temperatures between the triple point and the critical point. On further lowering of ε_{AB} , the demixing transition occurs in the liquid phase, and three different types of phase diagram topologies may appear.

The first (cf. part a of Fig. 1 in Ref. [3]) occurs when the vapor condenses into a demixed liquid only at temperatures up to the critical end point, T_{cep} , located below the critical point. At higher temperatures, the condensation leads to the formation of a mixed liquid, which undergoes a continuous demixing transition along a so-called λ line on the increase of density. The λ line originates at the critical end point, at which the critical liquids (A-rich and B-rich) coexist with a noncritical vapor. On the gradual decrease of the interaction strength between the unlike particles, the second case occurs. The vapor condenses into the demixed fluid at the temperatures up to the triple-point temperature, $T_{tr(v-m-l-dl)}$, at which the vapor coexists with the mixed (ml) and the demixed (dl) liquid phases (cf. part b of Fig. 1 in Ref. [3]). At the higher temperatures, the vapor condenses into a mixed liquid, which undergoes a demixing transition. This transition is of the first order, as long as the temperature is lower than the tricritical-point temperature, T_{trc} , at which the mixed and two demixed (A-rich and B-rich) liquid phases become critical. At higher temperatures, the demixing transition is continuous and takes place along the λ line. The vapor liquid coexistence terminates at the critical point again. For the sufficiently weak interaction between the unlike particles, another situation occurs. The vapor condenses into the demixed liquid all along the coexistence line, and this causes the λ line to intersect the vapor liquid coexistence right at the critical point. Therefore,

*andrzej.patrykiewicz@gmail.com

the critical point is replaced by the tricritical point, in which the vapor and A-rich and B-rich liquid phases all become critical (cf. part c of Fig. 1 in Ref. [3]).

The scenarios presented above may change considerably when geometrical nonadditivity ($\sigma_{AB} \neq \sigma_{AA}$) is taken into account. In the systems with $\varepsilon_{AB} = \varepsilon_{AA}$, only the packing effects matter, when σ_{AB} is varied. When $\sigma_{AB} < \sigma_{AA}$, the formation of AB pairs is favored, and leads to a local ordering that enhances the stability of the liquid with respect to the ideal mixture. In the case when $\sigma_{AB} > \sigma_{AA}$, one expects the pairs of the like particles to be preferentially formed and observes clustering of the like particles in the liquid [13,14]. The isothermal-isobaric (NPT) Monte Carlo studies have demonstrated [13,15] that, on the increase of σ_{AB} , the boiling point of such mixtures increases. This suggests that the liquid stability increases as well. However, the clustering of the like particles may lead to a microphase separation when σ_{AB} becomes large enough [14]. This phenomenon has also been observed in nonadditive hard-sphere mixtures [16].

In the mixtures with $\varepsilon_{AB} < \varepsilon_{AA}$, geometrical nonadditivity leads to important changes in the phases behavior of SBMs. Our Monte Carlo study of two-dimensional SBMs [4,8] has shown that geometrical nonadditivity considerably affects the properties of the λ line. When $\sigma_{AB} > \sigma_{AA}$, the liquid density along the λ line is nearly independent of temperature. Only the point at which the λ line intersects the vapor-liquid boundary changes with ε_{AB} (see Fig. 1 in Ref. [4]). In the case of $\sigma_{AB} < \sigma_{AA}$, the location of the demixing transition strongly depends on temperature. Therefore, it may either intersect the liquid-solid coexistence in the critical end point (see Fig. 4 in Ref. [4]) or lead to the appearance of closed-loop liquid-liquid immiscibility (see Fig. 10 in Ref. [8]). The same phenomenon was found by Almarza *et al.* [7] in three-dimensional SBMs.

The goal of this paper is to discuss the interplay between geometrical and energetic nonadditivity effects in a rather systematic way. In particular, we discuss the changes in the phase behavior of SBMs with negative ($\sigma_{AB} < \sigma_{AA}$) and positive ($\sigma_{AB} > \sigma_{AA}$) geometrical nonadditivity and with different values of $\varepsilon_{AB} \leq \varepsilon_{AA}$. In this study, the discussion is confined to the liquid-vapor transition and to the demixing phenomenon in the liquid phase. Nevertheless, we also present the estimations of the triple points for some of the systems considered in this work. In the following Sec. II, we describe the model and methods used. The Sec. III presents the results and discussion concerning the behavior of systems characterized by different parameters describing the interaction between the pairs of the like and unlike particles. The final Sec. IV includes a short summary and final remarks.

II. THE MODEL AND MONTE CARLO METHODS

We have considered the symmetrical mixtures consisting of components A and B, which interact via the truncated (12,6) Lennard-Jones potential

$$u_{ij}(r) = \begin{cases} 4\varepsilon_{ij}[(\sigma_{ij}/r)^{12} - (\sigma_{ij}/r)^6] & r \leq r_{\max} \\ 0 & r > r_{\max} \end{cases}, \quad (1)$$

where r is the distance between a pair of atoms and i and j mark the species A and B. In the symmetrical mixtures, the potential parameters describing interaction between the like particles

are the same, i.e., $\sigma_{AA} = \sigma_{BB} = \sigma$ and $\varepsilon_{AA} = \varepsilon_{BB} = \varepsilon$. The corresponding potential parameters for a pair of unlike atoms are given by

$$\sigma_{AB} = s\sigma \quad \text{and} \quad \varepsilon_{AB} = e\varepsilon, \quad (2)$$

where s and e are constants.

The potential is cut at the distance of $r_{\max} = 3.0s\sigma$, and σ is taken as the unit of length, while ε is used as the unit of energy. Thus, we use the reduced temperature, $T^* = kT/\varepsilon$, and the reduced chemical potentials of both species, $\mu_i^* = \mu_i/\varepsilon$, $i = A, B$. The potential energy is expressed in units of ε .

The Hamiltonian of the model reads

$$\begin{aligned} \mathcal{H}(\mathbf{R}_A, \mathbf{R}_B) = & \sum_{i < j}^{N_A} u_{AA}(r_{ij}) + \sum_{i < j}^{N_B} u_{BB}(r_{ij}) \\ & + \sum_{i=1}^{N_A} \sum_{j=1}^{N_B} u_{AB}(r_{ij}) - \mu_A^* N_A - \mu_B^* N_B. \end{aligned} \quad (3)$$

In the above, \mathbf{R}_A and \mathbf{R}_B are multidimensional vectors representing the positions of all atoms, $\mathbf{r}_{k_i} = (x_{k,i}, y_{k,i}, z_{k,i})$ of the components $k = A, B$ in the system [$\mathbf{R}_i = (\mathbf{r}_{1,i}, \mathbf{r}_{2,i}, \dots, \mathbf{r}_{N_i,i})$, $i = A$ or B].

In this work we have considered only the situation where the chemical potentials of both species are the same ($\mu_A^* = \mu_B^* = \mu^*$), so the Hamiltonian (3) becomes

$$\begin{aligned} \mathcal{H}(\mathbf{R}_A, \mathbf{R}_B) = & \sum_{i < j}^{N_A} u_{AA}(r_{ij}) + \sum_{i < j}^{N_B} u_{BB}(r_{ij}) \\ & + \sum_{i=1}^{N_A} \sum_{j=1}^{N_B} u_{AB}(r_{ij}) - \mu^* N, \end{aligned} \quad (4)$$

where $N = N_A + N_B$.

We have considered four series of systems. The first series (E1.0) involves the systems with $e = 1.0$ and different values of $s \in [0.6, 1.4]$. In this case, one expects a complete mixing in both liquid and solid phases. The main aim of our study has been to find out how the geometrical nonadditivity affects the properties and structure of the dense phases. Then, we have considered systems which are likely to exhibit a demixing transition in the liquid phase and assume that $e = 0.8$ (series E0.8), 0.7 (series E0.7), and 0.6 (series E0.6). In all these cases, the parameter s was varied within the range between 0.6 and 1.4. The case with $e = 0.9$ has not been taken into account, since we have not found any trace of a demixing transition in the liquid phase.

The model has been studied using Monte Carlo simulation methods in the grand-canonical ensemble [17–19]. Simulations have been carried out using cubic cells of the size $L \times L \times L$, with standard periodic boundary conditions. A vast majority of calculations have been carried out assuming that $L = 10$, but we have also used larger cells of $L = 12$ and 14.

The quantities recorded included the average numbers of particles A (N_A) and B (N_B), the average potential energy (per particle), $\langle e_{gg}^* \rangle$, and the radial distribution functions (rdfs), $g_{ij}(r)$, for $ij = AA, AB$, and BB . In order to locate the

demixing transition, we have calculated the order parameter

$$m = (N_A - N_B)/(N_A + N_B) \quad (5)$$

and its susceptibility

$$\chi_m(L) = \frac{L^2}{kT} [\langle m^2 \rangle - \langle m \rangle^2]. \quad (6)$$

Moreover, we have also recorded the probability distributions of the order parameter $[p(m)]$ and the distributions of total density $[p(\rho)]$. Calculations of these distribution functions have been carried out using hyperparallel tempering method [19]. All distributions $p(\rho)$ and $p(m)$ reported in this work have been normalized to unity.

Our calculations have been focused on the vapor-liquid part of the phase diagrams. The transitions leading to the formation of solid phases, either via the vapor-solid or the liquid-solid transition, cannot be reliably studied using grand-canonical Monte Carlo simulation. In the finite systems of constant volume and periodic boundary conditions, the effects of metastability are huge and hence it is not possible to estimate the locations of phase transitions. Besides, the system size is usually not compatible with the crystal structure, which also makes the study of solid formation somewhat difficult.

III. RESULTS AND DISCUSSION

A. Series E1.0

The systems belonging to this series are not expected to exhibit qualitatively different behavior when the parameter s is varied. As already mentioned in the Introduction, the changes in the properties of mixtures with a different s can be attributed entirely to the packing effects. From the earlier studies of Vlot *et al.* [20], it follows that the structure of solid phases depends strongly on the parameter s . In the region of s between 0.6 and 0.8, the regular cubic crystals of NaCl structure should be formed on freezing. Then, for $s = 0.9$, one can note the occurrence of the body centred cubic (bcc) structure of the CsCl type. For $s = 1.0$ and 1.1, the face centred cubic (fcc) mixed crystals are stable. For still larger s , the fcc structure with the like particles arranged in alternate (111) layers is expected to form. The behavior of liquid phases formed by the systems considered here has also been studied by Georgoulaki *et al.* [15] using Gibbs ensemble Monte Carlo simulation and by Vlot *et al.* [13] using NPT Monte Carlo simulation. However, those studies were carried out only at very few thermodynamic points (determined by pressure and temperature) and hence did not lead to the evaluation of full phase diagrams.

Our simulations have allowed us to estimate the phase diagrams for the systems with different s (see Fig. 1). Figure 1(a) presents the density-temperature projections of phase diagrams obtained for the systems with $s = 0.6, 0.7, 0.8$, and 0.9. According to the results obtained by Vlot *et al.* [20,21], the first three systems ($s = 0.6, 0.7$, and 0.8) are expected to crystallize into the cubic crystal of the NaCl type. It has also been shown that the Gibbs free energy of the solid attains minimum when $s = 0.7$. It is thus expected that the triple-point temperature reaches maximum for $s = 0.7$. From our simulations it follows that the triple-point temperature of the system with $s = 0.6$ is equal to $T_{tr} = 0.83 \pm 0.02$,

for $s = 0.7$ it is higher and equal to 0.97 ± 0.02 , while for $s = 0.8$ it appears at about 0.68 ± 0.02 . The calculations of radial distribution functions have also confirmed that these systems crystallize into the NaCl type structure. This has been illustrated by the results given in the lower panel to Fig. 2, which shows the radial distribution functions $g_{AA}(r)$ and $g_{AB}(r)$ obtained for the system with $s = 0.7$ at $T = 0.9$ and the chemical potential $\mu = -3.0$. The locations of subsequent maxima are consistent with the NaCl-type structure. The upper panel of Fig. 2 shows the rdfs obtained at the temperature $T = 1.0$, i.e., above the triple point. One should notice that the locations of subsequent maxima show a large tendency towards the appearance of AB pairs. This effect is larger (smaller) when the parameter s becomes lower (higher). Consequently, the density of the liquid gradually lowers with the increase of parameter s . Figure 1(a) also shows that the critical temperature gradually decreases, with the increase of the parameter s from 0.6 to 1.0.

In the case of $s = 0.9$, our simulation has also shown that the triple-point temperature seems to be located slightly below 0.65, and the crystal has the bcc structure of the same type, as occurs for CsCl (see the lower panel of Fig. 3). The radial distribution functions demonstrate also that the liquid does not possess such a well-developed structure, as observed in the systems with lower s .

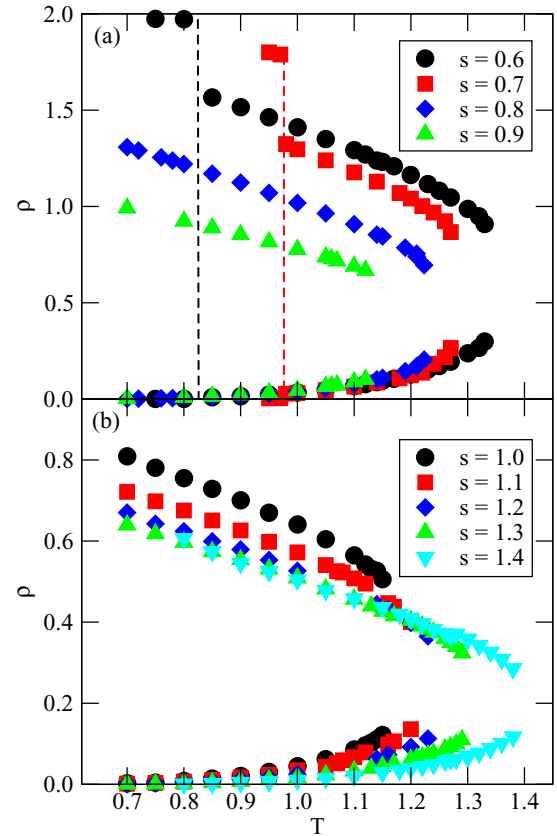


FIG. 1. Phase diagrams in the temperature-density plane for the systems characterized by $e = 1.0$ and different values of the parameter s , given in the figure. Panels (a) and (b) show the phase diagrams for $s < 1$ and $s \geq 1$. The vertical dashed lines in (a) denote the estimated locations of triple points for the systems with $s = 0.6$ and 0.7.

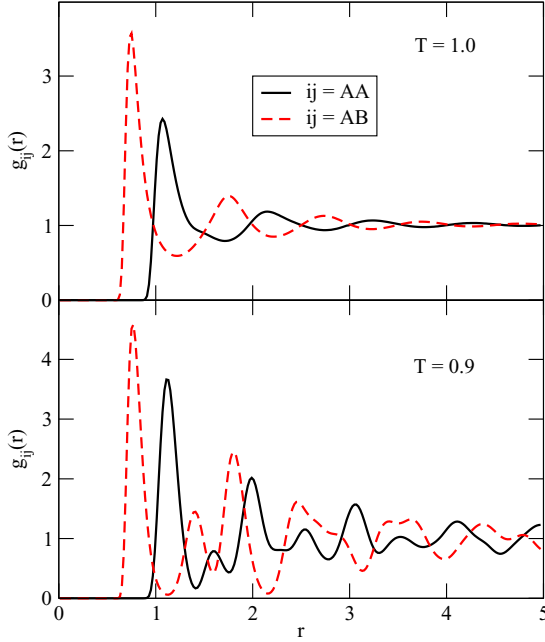


FIG. 2. The radial distribution functions $g_{AA}(r)$ and $g_{AB}(r)$ for the system with $e = 1.0$ and $s = 0.7$ at two temperatures, above (upper panel) and below (lower panel) the triple point and at the chemical potential $\mu = -3.0$.

The case of $s = 1.0$ corresponds to the ideal mixture, and its behavior should not differ from the one-component system. In particular, we have found that the critical temperature occurs at about $T_c = 1.18$, in agreement with the estimations of T_c for Lennard-Jones fluid with the truncated interaction

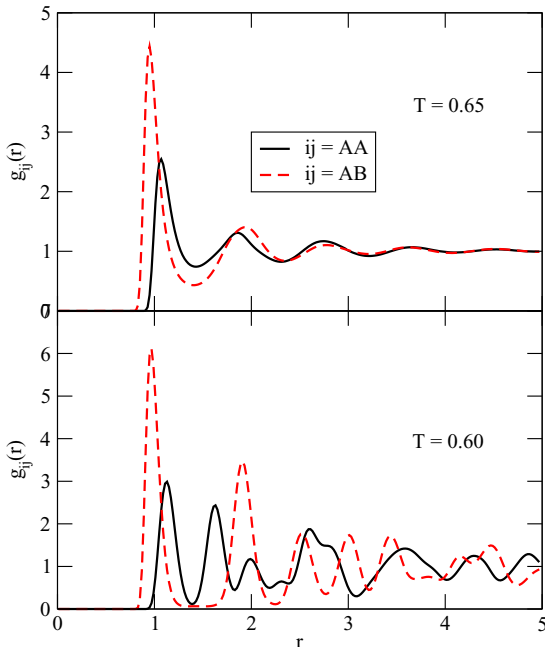


FIG. 3. The radial distribution functions $g_{AA}(r)$ and $g_{AB}(r)$ for the system with $e = 1.0$ and $s = 0.9$ at two temperatures, above (upper panel) and below (lower panel) the triple point and at the chemical potential $\mu = -3.0$.

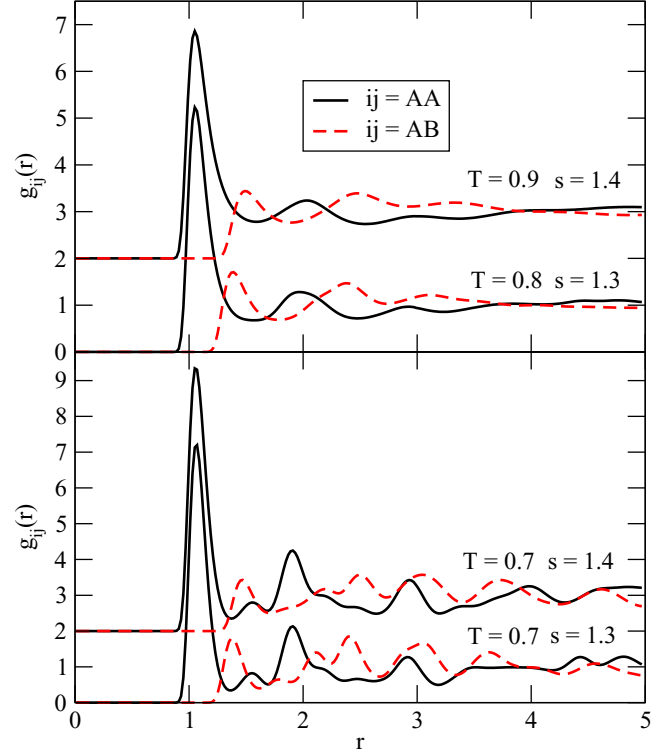


FIG. 4. The radial distribution functions $g_{AA}(r)$ and $g_{AB}(r)$ for the systems with $e = 1.0$ and $s = 1.3$ and 1.4 at the temperatures, above (upper panel) and below (lower panel) the freezing point and at the chemical potential $\mu = -4.0$.

potential [22]. This system is expected to crystallize into a fcc structure [20,21], and its triple point is equal to about $T_{tr} = 0.694$ [23].

When the parameter s increases above unity, we have found that the critical temperature also gradually increases, as has been shown in the phase diagrams depicted in Fig. 1(b). The observed increase of the critical temperature is associated with the gradual increase of the tendency to form aggregates consisting of the like particles. The formation of such aggregates has been observed in bulk SBMs by Vlot *et al.* [13], as well as in two-dimensional SBMs [24,25]. In the range of the parameter s considered here, the aggregation does not lead to a true phase separation but only to the formation of clusters of the like particles. The clustering is reflected in the behavior of radial distribution functions (see Fig. 4), which demonstrates that the formation of AB pairs is considerably suppressed in the liquid as well as in the solid phase. Our calculations have not allowed us to determine the structure of the solid phases and to estimate the locations of the triple points. Nevertheless, the results of Monte Carlo simulation suggest that the freezing temperature gradually increases with s .

B. Series E0.8

The phase behavior of systems belonging to the second series (S0.8) considerably differs, since the interaction between the unlike particles is weaker ($e = 0.8$), and one expects to observe a demixing transition in the liquid phase. However, the systems with sufficiently small values of $s = 0.6, 0.7$,

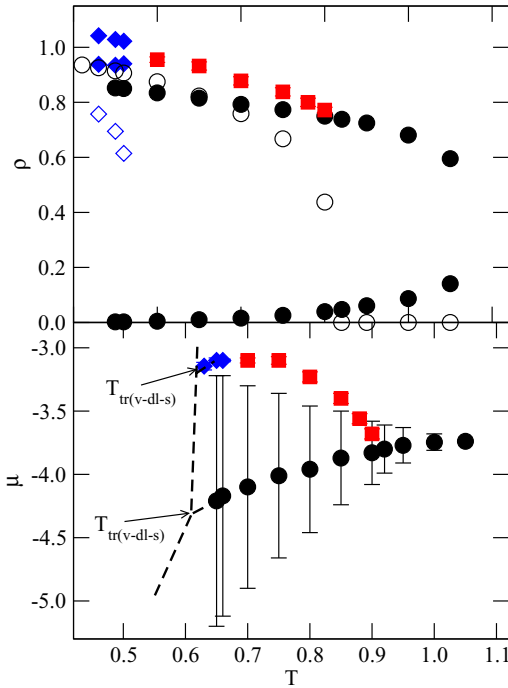


FIG. 5. The phase diagram in the temperature-density (upper panel) and temperature-chemical potential (lower panel) planes for the system with $e = 0.8$ and $s = 0.9$. Filled circles correspond to the vapor-liquid transition, filled squares (diamonds) represent the continuous (discontinuous) transition between the demixed and mixed liquid phases, while open circles and diamonds are the values of the order parameter m in the demixed liquid phase along the vapor-liquid and the demixed liquid-mixed liquid phase boundaries. The dashed lines are the expected phase boundaries in the low-temperature region. $T_{\text{tr}(v-dl-s)}$ and $T_{\text{tr}(dl-ml-s)}$ are the expected locations of triple points.

and 0.8 have been found to form only a mixed liquid phase, so their phase diagrams are qualitatively the same as those found for the systems belonging to the series S1.0. This can be attributed to the fact that for small values of the parameter s , the formation of AB pairs is strongly favored. Thus, large packing effects dominate over the energetic effects.

An increase of s to 0.9 diminishes the role of packing effects, and the demixing transition has been found to occur over a limited range of sufficiently low temperatures and densities. The phase diagram for this system is given in Fig. 5. It shows that at sufficiently low temperatures, below the critical end point located at about $T_{\text{cep}} = 0.91$, the vapor condenses into the demixed liquid. The open circles in the upper panel of Fig. 5 show the changes of the order parameter m along the phase boundary at the liquid side of vapor-liquid coexistence, and it is quite evident that the liquid is mixed above T_{cep} . On the increase of density, the demixed liquid undergoes a transition into the mixed liquid of higher density. This transition is of the first order at the temperatures lower than the tricritical temperature, equal to about $T_{\text{trc}} = 0.68 \pm 0.02$, and becomes continuous at the temperatures between T_{trc} and T_{cep} . Open diamonds in the upper panel of Fig. 5 give the values of the order parameter m in the low-density demixed liquid phase at the transition points.

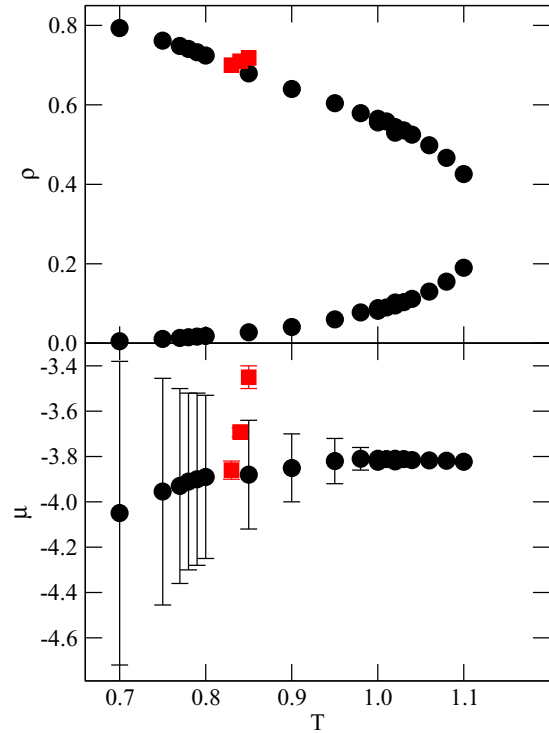


FIG. 6. The phase diagram in the temperature-density (upper panel) and temperature-chemical potential (lower panel) planes for the system with $e = 0.8$ and $s = 1.0$. Filled circles correspond to the vapor-liquid transition and filled squares represent the continuous transition between the demixed and mixed liquid phases.

When the temperature becomes low enough, the line of the vapor-demixed liquid transition is bound to terminate at the triple point, $T_{\text{tr}(v-dl-s)}$, in which the demixed liquid (dl), vapor (v), and solid (s) coexist. Also, the coexistence between the dl and ml liquids has to terminate in the triple point, $T_{\text{tr}(dl-ml-s)}$, in which the two liquid phases coexist with a solid. This has been marked by the dashed lines in the lower panel of Fig. 5. We have to emphasize that these lines are only a guess, since we have not been able to determine the locations of liquid-solid transition points due to the extremely large metastability effects.

One can expect that the freezing of a demixed liquid, occurring at the temperatures below $T_{\text{tr}(dl-ml-s)}$, leads to the formation of the demixed solid. On the other hand, the freezing of a mixed liquid may produce a mixed or demixed solid. Thus, it is likely that the solid undergoes the transition between demixed and mixed states as the temperature increases.

The phase diagram topology changes completely, when the parameter s increases to unity (see Fig. 6). In this case, the vapor-liquid condensation leads to the formation of demixed liquid at the temperatures up to the critical end point at $T_{\text{cep}} = 0.83$. At higher temperatures, the continuous demixing transition takes place in the liquid phase along the λ line. Although we have estimated only a very few points along the λ line, it seems quite possible that it may meet the liquid-solid coexistence at the upper critical end point. This prediction is based on the observation that the λ line exhibits a strong dependence on temperature. We should recall that in the case of two-dimensional SBMs, the systems with $s = 1$ were found

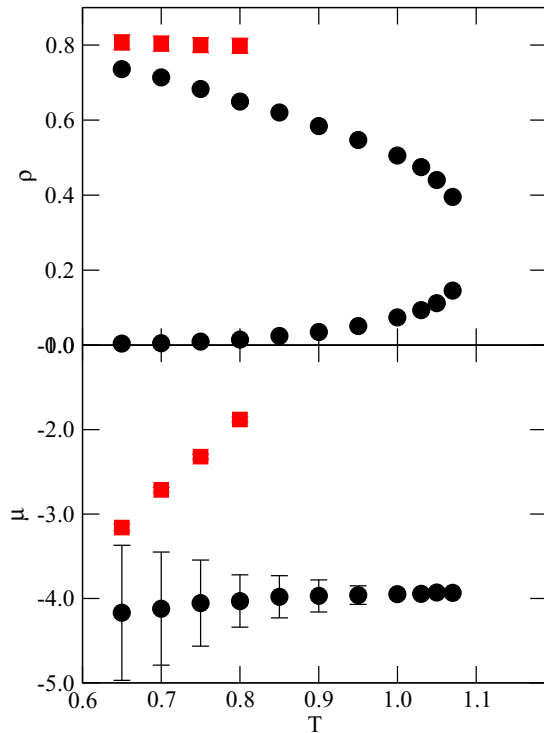


FIG. 7. The phase diagram in the temperature-density (upper panel) and temperature-chemical potential (lower panel) planes for the system with $e = 0.8$ and $s = 1.1$. Filled circles correspond to the vapor-liquid transition and filled squares represent the continuous transition between the demixed and mixed liquid phases.

to exhibit the presence of the lower and upper critical end points [5].

When the parameter s exceeds unity, one expects the mixtures to show the enhanced tendency towards demixing in the liquid phase. In the case of $e = 1.0$, the liquid phase in systems with $s > 1$ exhibits agglomeration of the like particles. When the interaction between the unlike particles becomes weaker than the interaction between the like particles, as in the presently discussed systems, the aggregation of the like particles should be stronger and favor demixing. The situation appears to be more complex, however. Already for $s = 1.1$, the phase diagram topology (see Fig. 7) differs than in the case of $s = 1$ (cf. Fig. 6). The vapor condenses into a mixed liquid, even at quite low temperatures, and the vapor-liquid transition terminates in a critical point located at $T_c = 1.08 \pm 0.01$. The liquid undergoes a continuous demixing transition but only at sufficiently high densities. From our results it seems plausible that the onset of the λ line occurs at the liquid side of the liquid-solid coexistence. At this point, we should mention again that our earlier study of two-dimensional SBMs [4,5] has demonstrated that the magnitude of the parameter s has a big influence on the behavior of λ line. In particular, it has been shown that for sufficiently large $s > 1$, the density at which the demixing transition takes place is nearly independent of temperature. Moreover, in the systems that do not show a sufficiently strong tendency towards demixing, the onset of the λ line is shifted to lower temperatures and higher densities. It is then possible that the λ line begins at the liquid-solid

coexistence [5]. It seems to be the case when $e = 0.8$ and $s = 1.1$. Although we have not estimated the location of the triple point and the liquid-solid coexistence, nevertheless the obtained data have demonstrated that the triple point and the onset of the λ line appear below $T = 0.65$.

Qualitatively similar behavior has been established for the system with $s = 1.2$ but with the onset of the λ line shifted to still higher temperatures. The simulation performed at $T = 0.75$ and 0.80 has shown that the mixed liquid freezes into the also mixed solid. Thus, the onset of the demixing transition has to occur at still higher temperatures. For still larger values of $s = 1.3$ and 1.4 , we have not found the demixing transition at all. It seems that the onset of λ line is either located at the liquid side of the liquid-solid coexistence at very high temperatures or the demixing transition in the liquid does not occur at all. Namely, it is possible that the demixing occurs at the densities higher than the densities along the liquid side of the liquid-solid coexistence. If that is the case, then the demixing should occur in the solid phase only.

C. Series E0.7

The next series of systems, with $e = 0.7$, should exhibit still higher tendency towards phase separation. From the earlier studies of Wilding *et al.* [3], it is known that when $s = 1$ the demixing transition accompanies the vapor-liquid

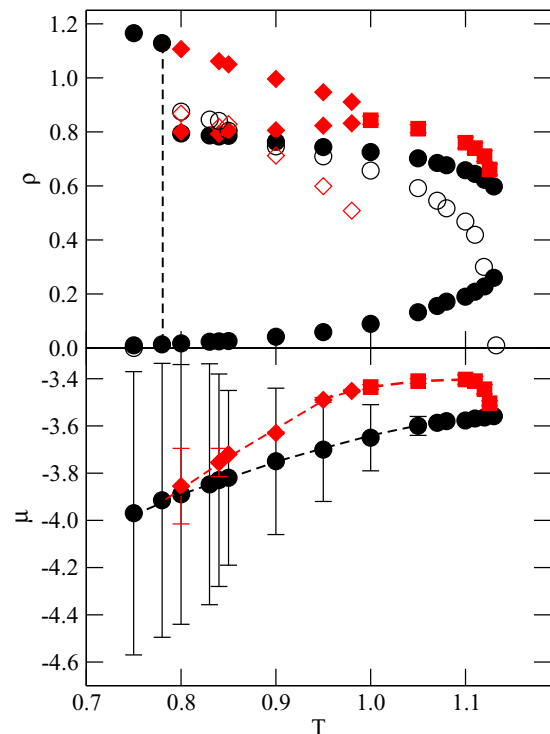


FIG. 8. The phase diagram in the temperature-density (upper panel) and temperature-chemical potential (lower panel) planes for the system with $e = 0.7$ and $s = 0.8$. Filled circles correspond to the vapor-liquid transition, and filled squares (diamonds) represent the continuous (discontinuous) transition between the demixed and mixed liquid phases. Open circles and diamonds are the values of the order parameter m in the demixed liquid phase along the vapor-liquid and the demixed liquid-mixed liquid phase boundaries.

condensation up to the critical end-point temperature of about $T_{cep} = 0.96$ [3]. At higher temperatures, the demixing transition is continuous and occurs along the λ line. Our calculations have confirmed this behavior very well. In particular, the critical point of the vapor-liquid condensation has been found to be located at $T_c = 1.045 \pm 0.005$, in good agreement with the results given in Ref. [3]. Also, the estimated temperature of the critical end point ($T_{cep} = 0.96 \pm 0.05$) conforms with the results of Wilding *et al.* [3].

The systems with large negative geometrical nonadditivity ($s = 0.6$ and 0.7) have not been found to undergo a demixing transition in the liquid phase, but this transition takes place when $s = 0.8$. In this case, the phase diagram (see Fig. 8) is qualitatively similar to the previously discussed case of $e = 0.8$ and $s = 0.9$ (cf. Fig. 6). However, the critical end point as well as the tricritical point exhibit a shift towards higher temperatures, and $T_{cep} = 1.125$ and $T_{trc} = 0.99$. Figure 9(a) presents the probability distribution functions $p(\rho)$ and $p(m)$ at the temperature $T = 1.13$ just below the critical point ($T_c \approx 1.14$) and shows that the liquid phase is not demixed. On the other hand, the probability distribution $p(m)$ recorded at the vapor-liquid coexistence at a slightly lower temperature

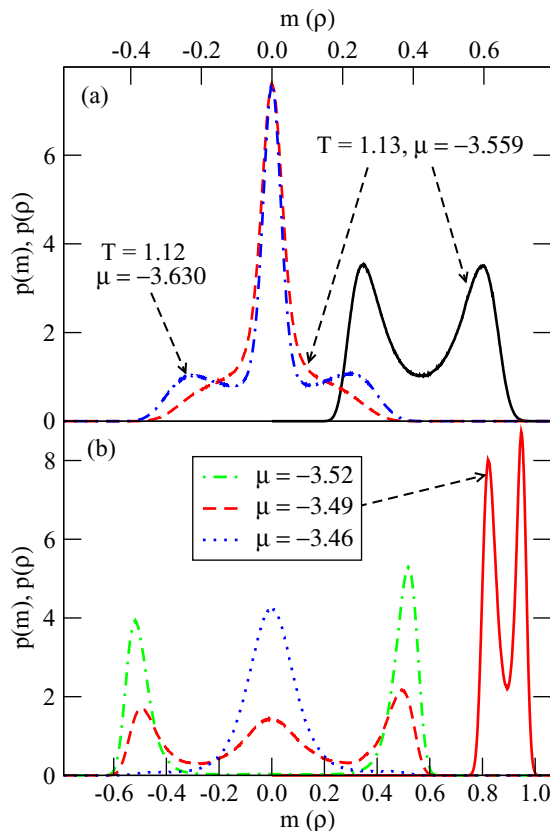


FIG. 9. The probability distribution functions $p(m)$ and $p(\rho)$ for the system with $e = 0.7$ and $s = 0.8$. Panel (a) shows the $p(m)$ distributions at $T = 1.12$ and 1.13 along the vapor liquid coexistence and the distribution $p(\rho)$ at $T = 1.13$ (the solid line). Panel (b) shows the distributions $p(m)$ recorded at $T = 0.95$ at three different values of the chemical potential below at and above the first-order demixing transition in the liquid and the distribution $p(\rho)$ at the coexistence between the demixed and mixed liquids at $T = 0.95$ (the solid line).

of $T = 1.12$ [also shown in Fig. 9(a)] demonstrates that the vapor condenses into the demixed liquid. Figure 9(b) shows the probability distribution functions $p(\rho)$ and $p(m)$ recorded at $T = 0.95$ in the region of the transition between the demixed and mixed liquid phases. The density distribution is bimodal, indicating that the demixing transition is of the first order. One readily notes that the liquid at μ below the transition point is demixed, while the high-density liquid at μ above the transition point is mixed. The only qualitatively new feature is the appearance of the triple point, located at $T_{v,ml,dl} = 0.78 \pm 0.01$, at which the vapor coexists with mixed and demixed liquids. At the temperatures below the triple point, the vapor condenses into the mixed liquid. Large metastability effects have not allowed, however, for the estimation of the triple point at which the vapor, the mixed liquid, and the solid phases coexist.

An increase of the parameter s to 0.9 changes the phase behavior, and the phase diagram (see Fig. 10) is similar to the one obtained for $e = 0.8$ and $s = 0.9$. The difference is that the vapor to liquid condensation is accompanied by the demixing transition at all temperatures from the triple point up to the tricritical point, which replaces the critical point. On the increase of density, the demixed liquid undergoes the transition to the mixed liquid. At low temperatures, this transition starts at the triple point [$T_{tr(dl-m-l-s)}$], in which the demixed and mixed

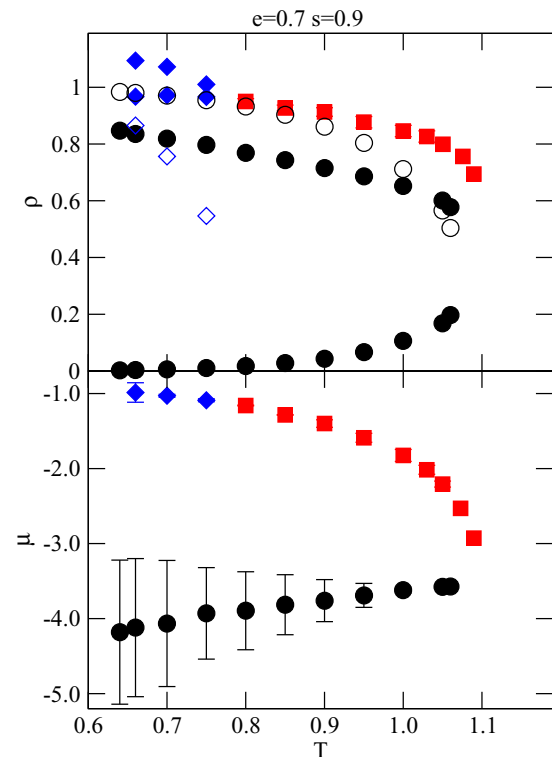


FIG. 10. The phase diagram in the temperature-density (upper panel) and temperature-chemical potential (lower panel) planes for the system with $e = 0.7$ and $s = 0.9$. Filled circles correspond to the vapor-liquid transition, and filled squares (diamonds) represent the continuous (discontinuous) transition between the demixed and mixed liquid phases. Open circles and diamonds are the values of the order parameter m in the demixed liquid phase along the vapor-liquid and the demixed liquid-mixed liquid phase boundaries.

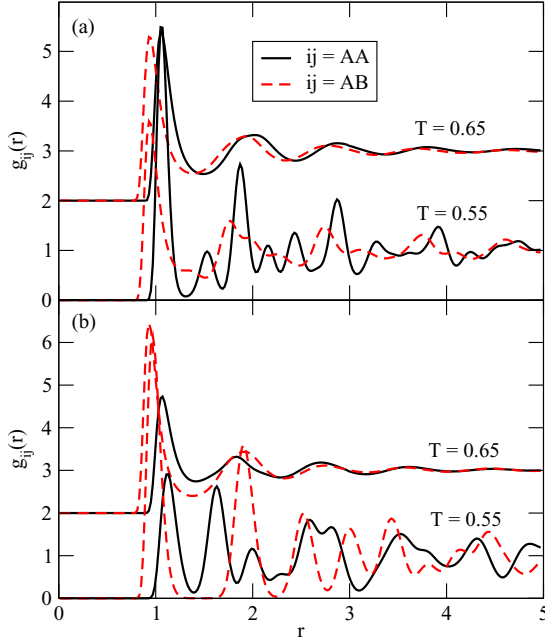


FIG. 11. The radial distribution functions $g_{AA}(r)$ and $g_{AB}(r)$ for the system with $e = 0.7$ and $s = 0.9$ at two temperatures, above and below the freezing point and at the chemical potential $\mu = -1.2$ (a) and -0.8 (b).

liquid phases coexist with the solid. The demixed-to-mixed transition in the liquid is of the first order at the temperatures up to the lower tricritical point, located at about $T_{l, \text{trc}} = 0.76$, being the onset of the λ line. The λ line exhibits a loop and terminates at the upper tricritical point at the temperature of about $T_{u, \text{trc}} = 1.075 \pm 0.005$. Although we have not been able to locate the vapor-liquid-solid and the demixed liquid-mixed liquid-solid triple points, nevertheless we could evaluate the radial distribution functions for the solid phases formed due to freezing of the demixed and mixed liquid phases. Figure 11(a) shows the rdfs obtained at two different temperatures above and below the freezing at $\mu = -1.2$, i.e., in the region in which the liquid is demixed. It appears that the solid phase is also demixed. Therefore, the radial distribution functions $g_{AB}(r)$ do not provide any meaningful information, since there are only very few AB pairs. On the other hand, the freezing of the mixed liquid results in a mixed solid, and the corresponding rdfs calculated at $\mu = -0.8$ are given in Fig. 11(b). From the locations of subsequent maxima, we can state that the demixed solid has the fcc structure, while the mixed solid has the bcc structure.

When the geometrical nonadditivity becomes positive ($s > 1$), the phase behavior is different than in the previously discussed case of $e = 0.8$. When $s = 1.1$, the system behaves similarly as in the case of $s = 1$, i.e., the continuous demixing occurs along the λ line originating at the critical end point located at the vapor-liquid coexistence at the temperature of about $T_{\text{cep}} = 0.84$. One should note that the critical end point is considerably lower than in the case of $s = 1$ ($T_{\text{cep}} = 0.96$). This demonstrates that entropic effects are strong and lower the stability of the demixed phase. Our calculations suggest that the critical point of the vapor-liquid condensation occurs at the temperature $T_c = 1.025 \pm 0.01$, i.e., slightly lower than in the

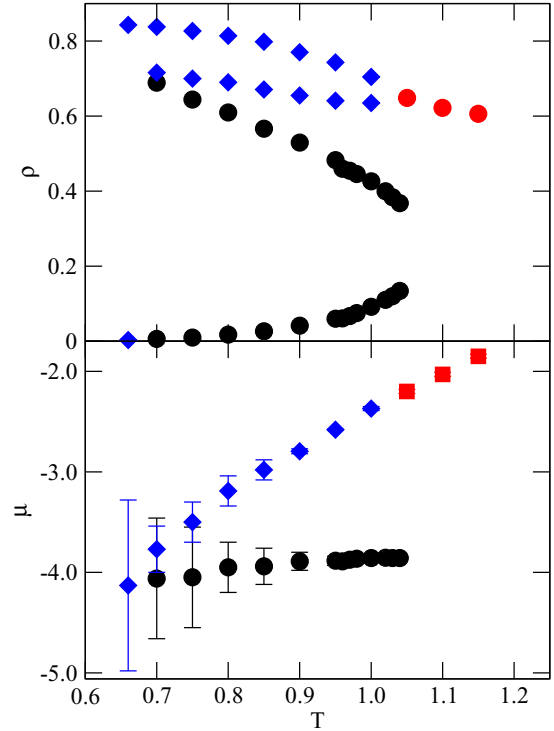


FIG. 12. The phase diagram in the temperature-density (upper panel) and temperature-chemical potential (lower panel) planes for the system with $e = 0.7$ and $s = 1.2$. Filled circles correspond to the vapor-liquid transition, and filled squares (diamonds) represent the continuous (discontinuous) transition between the demixed and mixed liquid phases.

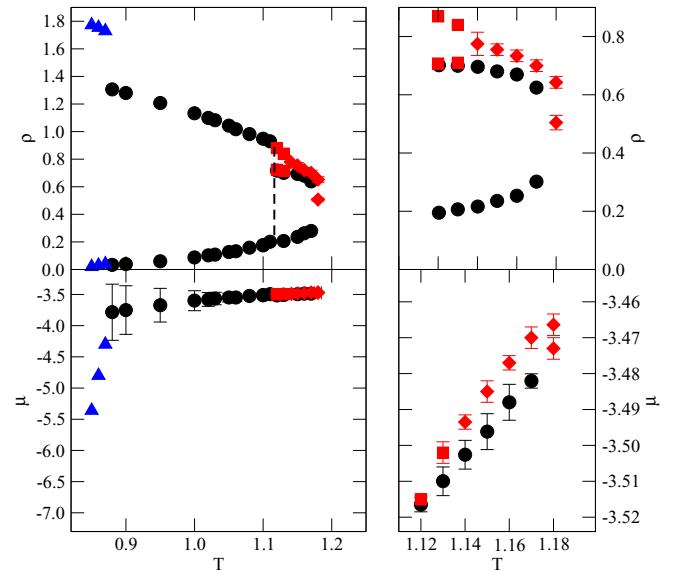


FIG. 13. The phase diagram in the temperature-density (upper panels) and temperature-chemical potential (lower panels) planes for the system with $e = 0.6$ and $s = 0.7$. Filled circles correspond to the vapor-liquid transition, filled squares (diamonds) represent the continuous (discontinuous) transition between the demixed and mixed liquid phases, and filled triangles show the vapor-mixed solid coexistence points. The vertical dotted line in the left upper panel shows the location of the triple point at which the vapor coexists with the demixed and mixed liquid phases.

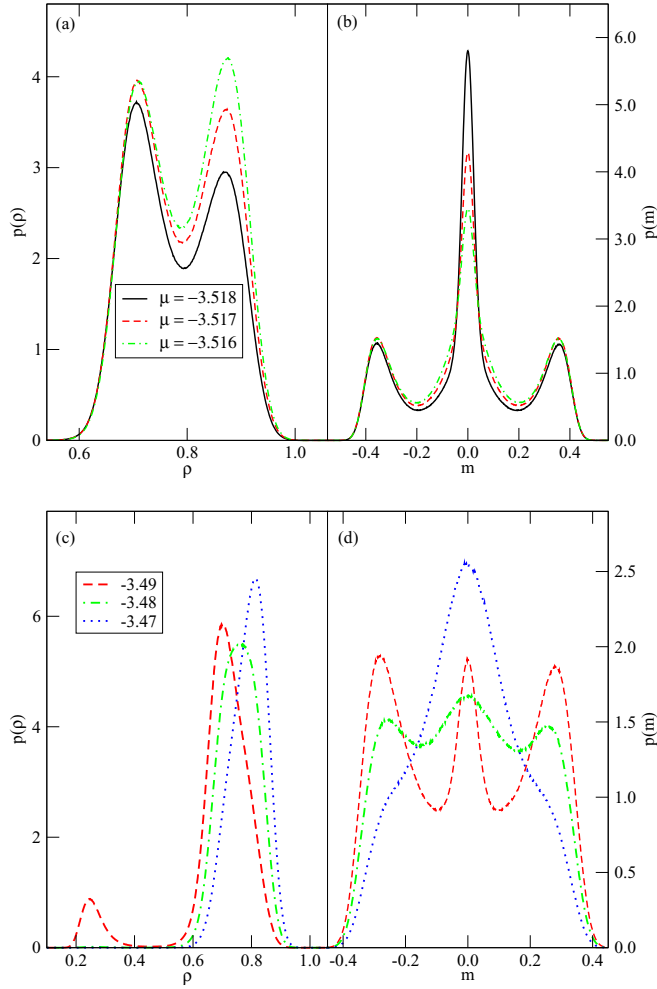


FIG. 14. The probability distribution functions $p(\rho)$ [(a) and (c)] and $p(m)$ [(b) and (d)] for the system with $e = 0.6$ and $s = 0.7$.

case of $s = 1$. Similarly to the case of $e = 0.8$ and $s > 1$, the density along the λ line exhibits only a very weak dependence on temperature. One expects that a further increase of the parameter s should cause a shift of the onset of the demixing transition to still lower temperatures. Indeed, when $s = 1.2$, the onset of demixing transitions occurs at the temperature of about 0.67 (see Fig. 12) but at the triple point rather than at the critical end point. At the triple point, the demixed and mixed liquids are in equilibrium with the vapor. Above the triple point, the demixing transition is discontinuous up to the tricritical point located at $T_{\text{trc}} = 1.03 \pm 0.02$. At still higher temperatures, we find a λ line. A further increase of the parameter s value to 1.3 and 1.4 causes the onset of the demixing to occur also at the triple point but at the liquid solid coexistence. Thus, at the triple point, the demixed and mixed liquids coexist with a solid. In all these systems, the vapor-mixed liquid coexistence terminates at the critical points that occur at slightly increasing temperatures, when the value of the parameter s increases from 1.1 to 1.4.

D. Series E0.6

The systems with $e = 0.6$ exhibit a very strong tendency towards demixing. However, we have not found any trace of

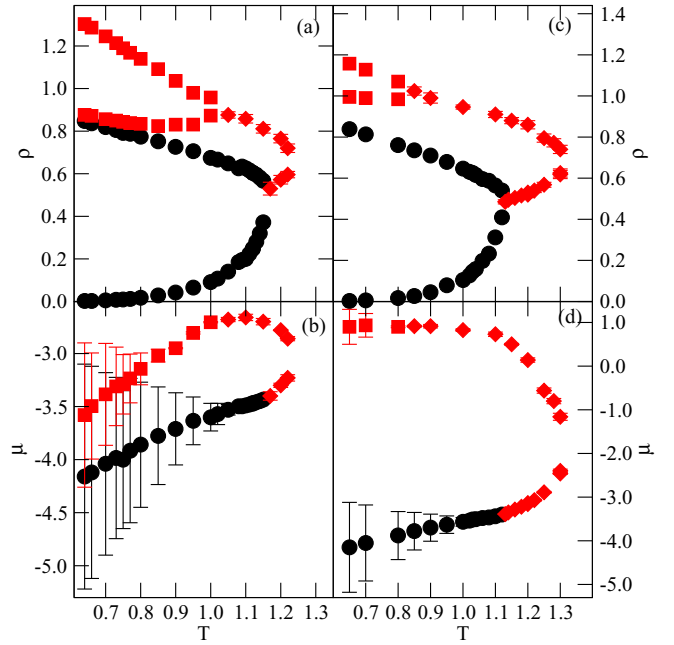


FIG. 15. The phase diagrams in the temperature-density [(a) and (c)] and temperature-chemical potential [(b) and (d)] planes for the systems with $e = 0.6$ and $s = 0.8$ [(a) and (b)] and $e = 0.6$ and $s = 0.9$ [(c) and (d)]. Filled circles correspond to the vapor-liquid transition, and filled squares (diamonds) represent the continuous (discontinuous) transition between the demixed and mixed liquid phases.

demixing in the liquid phase for $s = 0.6$. The vapor-liquid coexistence starts at the triple point, at which both the liquid and solid phases are mixed [$T_{\text{tr}(v\text{-ml},ms)} \approx 0.80$] and ends at the critical point at $T_c = 1.23 \pm 0.01$. The mixed solid forms crystals of the NaCl structure [20]. This has been confirmed by the calculations of the radial distribution functions. Although the emerging from the rdfs ordering is not perfect, the locations of subsequent maxima are consistent with the assumed structure.

When the parameter $s = 0.7$, the phase diagram topology changes and becomes qualitatively the same as in the case of $e = 0.7$ and $s = 0.8$. However, the demixing transition occurs only over a very narrow range of temperatures, as shown in Fig. 13. The presence of demixing transition has been found due to calculations of probability distribution functions $p(\rho)$ and $p(m)$, which are presented in Fig. 14. Figures 14(a) and 14(b) demonstrate the first-order demixing transition, which takes place between the triple-point temperature $T_{\text{tr}(v\text{-ml-dl})} = 1.11 \pm 0.005$ and the lower tricritical-point temperature $T_{l,\text{trc}} = 1.135 \pm 0.005$. Then, in Figs. 14(c) and 14(d), we have presented the examples of the probability distribution functions characteristic of the continuous demixing transition at the temperature above $T_{l,\text{trc}}$. It should be also noted that the solid phase structure is the same as in the case of $s = 0.6$, and the triple point occurs at $T_{\text{tr}(v\text{-ml-ms})} = 0.90 \pm 0.01$.

The systems with $s = 0.8$ and 0.9 exhibit qualitatively similar behavior as the system with $e = 0.7$ and $s = 0.9$, and the corresponding phase diagrams are presented in Fig. 15.

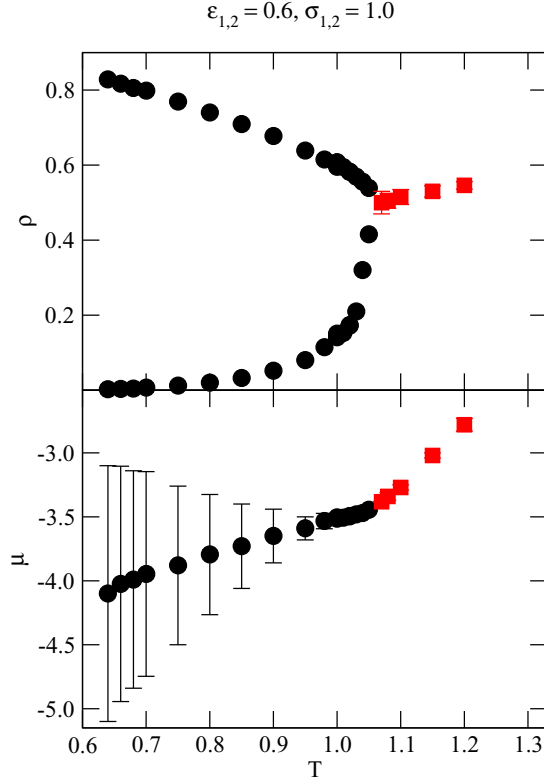


FIG. 16. The phase diagram in the temperature-density (upper panel) and temperature-chemical potential (lower panel) planes for the system with $e = 0.6$ and $s = 1.0$. Filled circles correspond to the vapor-liquid transition and filled squares represent the continuous transition between the mixed and demixed liquid phases.

There is, however, a qualitative difference in the phase behavior of these two systems. Namely, in the case of $s = 0.8$, the solid phase appears to be mixed and exhibits the NaCl structure. On the other hand, the system with $s = 0.9$ has been found to freeze into the demixed solid phase of the fcc structure.

A high tendency towards demixing causes, in the system with $s = 1.0$, the vapor to condense into a demixed liquid at all temperatures up to the tricritical point. The phase diagram for this system has been presented in Fig. 16.

In the case of $s \geq 1.1$, the phase behavior seems to be qualitatively the same as the one observed for $e = 0.7$ and $s = 1.2$. However, when $s = 1.1$, we have not been able to observe the first-order demixing transition. Therefore, the temperature difference between the triple point, in which the vapor coexists with the mixed and demixed liquid phases, and the tricritical point is either very small or the demixing transition starts in the critical end point. We have performed some additional calculations for the systems with $s = 1.05$ and 1.15 and have not been able to find any trace of the first-order demixing transition. The evaluated phase diagrams for the systems characterized by different values of the parameter s have allowed us to construct some sort of a global phase diagram (see Fig. 17), which shows the changes of different characteristic temperatures occurring alongside the changes of the geometric nonadditivity changes. Taking into account the results given in Fig. 17, we can assume that the systems with $s = 1.05$, 1.1 , and 1.15 do not exhibit the first-order demixing

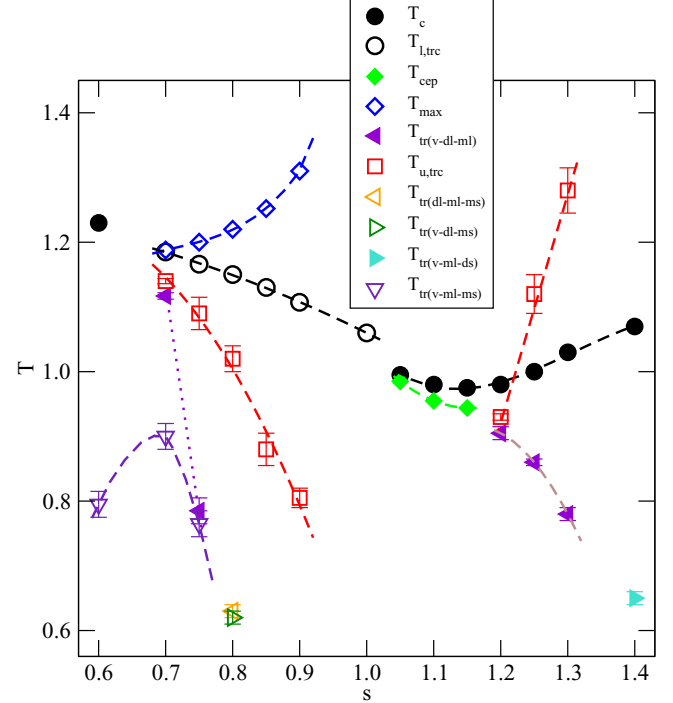


FIG. 17. The global phase diagram for the systems with $e = 0.6$ and different values of the parameter s . Here we have presented the locations of critical points (T_c), the upper and lower tricritical points ($T_{u,trc}$ and $T_{l,trc}$), the critical end points (T_{cep}), different triple points ($T_{t,v-dl-ml}$, $T_{t,v-dl-ms}$, $T_{t,v-dl-ds}$, $T_{t,v-ml-ms}$, $T_{t,v-ml-ds}$, and $T_{t,dl-ml-ms}$), and the maximum temperature, at which the demixing transition occurs in systems exhibiting the lower and upper tricritical points (T_{max}). The lines are only a guide to the eye.

transition at all, and the λ line starts at the critical end point. Figure 17 also shows that in the systems with $s \in [0.7, 0.9]$, in which the λ line exhibits a close loop, the range of temperatures over which the demixing transition occurs rapidly increases, with the parameter s approaching unity.

IV. SUMMARY AND FINAL REMARKS

We have performed extensive Monte Carlo simulations for three-dimensional symmetrical mixtures characterized by different parameters representing the interaction between the unlike species. We have focused on the systems with $e \leq 1.0$, and $s \in [0.6, 1.4]$.

The systems with $e = 1.0$ do not phase separate and the evaluated phase diagrams have shown that the critical temperature of the vapor-liquid condensation exhibits the minimum, when $s = 1.0$. In the case of negative nonadditivity ($s < 1$), the increase of the critical point with the decrease of the parameter s can be attributed to growing tendency towards the formation of AB pairs. This causes the liquid to exhibit a partial short-ranged ordering, which increases the liquid phase stability and leads to a higher density of the liquid phase. The appearance of the short-ranged ordering is also enhanced by the fact that the potential well of the AB interaction becomes narrower, when the value of the parameter s becomes lower. The systems with positive nonadditivity ($s > 1$) also show a

gradual increase of the critical temperature with the increase of the parameter s , but the mechanism leading to a higher stability of the liquid phase differs. An increasing value of the parameter s widens the potential well of the AB interactions so rather large deviations from the optimum distance are possible without much energy loss. Since the potential well of the AA (BB) interaction is narrower, the formation of pairs of like particles is favored. As a consequence, such systems show an increasing tendency towards the clustering of the like particles in the liquid phase, when the value of the parameter s increases. This clustering allows the system to attain a larger density than it would appear, if AB pairs were dominating.

When the interaction between A and B particles is sufficiently lower than the interaction between a pair of the like particles ($e < 1$), one can observe the demixing transition in the liquid phase. We have demonstrated that the geometric nonadditivity considerably influences the tendency towards demixing. Taking into account the results obtained for the systems with $e = 1$, one can expect that the lowering of s should suppress the tendency towards demixing in the systems with $e < 1$. The results presented in this work support that prediction quite well. When $e = 0.8$, the systems with $s < 0.9$ do not show a demixing transition in the liquid at all. On lowering e to 0.7, such limiting value of the parameter s decreases to about 0.8, while in the case of $e = 0.6$, it remains slightly below 0.7. We have demonstrated that the mixtures with $e < 1$ and negative geometrical nonadditivity show a rather complex phase behavior. In particular, it appears that the demixing transition occurs only over a certain range of temperatures between the triple-point temperature $T_{tr(v-m-l-d)}$, at which the vapor coexists with a mixed and demixed liquid and the critical end point located at the liquid side of the

vapor-liquid coexistence, as it has been found for the systems with $e = 0.8$ and $s = 0.9$ and with $e = 0.7$ and $s = 0.8$. It may also happen that the λ line exhibits a close loop behavior and terminates at the tricritical point which replaces the vapor-liquid critical point. This has been found to be the case in several systems, e.g., characterized by $e = 0.6$ and $s = 0.7$, 0.8, or 0.9 as well as $e = 0.7$ and $s = 0.9$. In all these cases, the demixed liquid of lower density undergoes a transition to a denser mixed liquid phase on the increase of the chemical potential.

On the other hand, the systems with the positive geometrical nonadditivity ($s > 1$) might have been expected to show a higher tendency towards demixing than the systems with $s = 1$. However, our calculations have demonstrated that it is not the case. For example, in the case of $e = 0.8$ and $s = 1.1$, the vapor-liquid transition is not accompanied by the phase separation at the temperatures down to the triple point. The λ line starts at the critical end point located at the liquid side of the liquid-solid coexistence. In the system with $e = 0.7$ and $s = 1.1$, the onset of the λ line is located along the vapor-liquid coexistence at the critical end point, but $T_{cep} = 0.84$ is considerably lower than $T_{cep} = 0.96$ of the system with $e = 0.7$ and $s = 1$. The systems with $s \geq 1.2$ and $e = 0.8, 0.7$ and 0.6 do not show the demixing transition along the vapor-liquid coexistence. The demixing transition occurs, but only when the liquid density becomes high enough. Demixed liquid is the phase of higher density due to the already-mentioned properties of the interaction potentials for AA and AB pairs.

In conclusion, we should mention that the present results agree quite well with our earlier studies of the two-dimensional symmetrical mixtures [4,5,8,24].

-
- [1] P. H. van Konynenburg and R. L. Scott, *Philos. Trans. Roy. Soc. London* **A298**, 495 (1980).
- [2] J. S. Rowlinson and F. L. Swinton, *Liquids and Liquid Mixtures*, 3rd ed. (Butterworths, London, 1982).
- [3] N. B. Wilding, F. Schmid, and P. Nielaba, *Phys. Rev. E* **58**, 2201 (1998).
- [4] S. Materniak, A. Patrykiewicz, and S. Sokołowski, *J. Chem. Phys.* **133**, 244501 (2010).
- [5] A. Patrykiewicz and S. Sokołowski, *Phys. Rev. E* **81**, 012501 (2010).
- [6] S. Roy, S. Dietrich, and F. Höfling, *J. Chem. Phys.* **145**, 134505 (2016).
- [7] N. G. Almarza, E. Enciso, M. F. García, M. A. González, and F. J. Bermejo, *Phys. Rev. E* **64**, 012501 (2001).
- [8] S. Materniak, A. Patrykiewicz, and W. Rżysko, *Phys. Rev. E* **87**, 062306 (2013).
- [9] S. K. Das, J. Horbach, K. Binder, M. E. Fisher, and J. V. Sengers, *J. Chem. Phys.* **125**, 024506 (2006).
- [10] D. Pini, M. Tau, A. Parola, and L. Reatto, *Phys. Rev. E* **67**, 046116 (2003).
- [11] D. Woywod and M. Schoen, *Phys. Rev. E* **73**, 011201 (2006).
- [12] N. B. Wilding, *Phys. Rev. E* **67**, 052503 (2003).
- [13] M. J. Vlot, C. Classen, H. E. A. Huitema, and J. P. Van der Eerden, *Molec. Phys.* **91**, 19 (1997).
- [14] J. N. Canangia Lopes, *Phys. Chem. Chem. Phys.* **4**, 949 (2002).
- [15] A. M. Georgoulaki, I. V. Ntouro, D. P. Tassios, and A. Z. Panagiotopoulos, *Fluid Phase Equil.* **100**, 153 (1994).
- [16] M. Rovere and G. Pastore, *J. Phys., Condens Matter* **6**, A163 (1994).
- [17] D. Frenkel and B. Smit, *Understanding Molecular Simulation: From Algorithms to Applications* (Academic Press, San Diego, 1996).
- [18] M. P. Allen and D. J. Tildesley, *Computer Simulation of Liquids* (Oxford University Press, Oxford, 1987).
- [19] D. P. Landau and K. Binder, *A Guide to Monte Carlo Simulation in Statistical Physics* (Cambridge University Press, Cambridge, 2000).
- [20] M. J. Vlot, J. C. van Miltenburg, H. A. J. Oonk, and J. P. van der Eerden, *J. Chem. Phys.* **107**, 10102 (1997).
- [21] M. J. Vlot, H. E. A. Huitema, A. de Vooy, and J. P. van der Eerden, *J. Chem. Phys.* **107**, 4345 (1997).
- [22] E. S. Loscar, C. G. Ferrara, and T. S. Grigera, *J. Chem. Phys.* **144**, 134501 (2016).
- [23] E. A. Mastny and J. J. de Pablo, *J. Chem. Phys.* **127**, 104504 (2007).
- [24] A. Patrykiewicz and S. Sokołowski, *J. Phys. Chem. B* **114**, 396 (2010).
- [25] M. J. Vlot and J. P. van der Eerden, *J. Chem. Phys.* **109**, 6043 (1998).